LABORATORY EXAFS SPECTROMETER, PRINCIPLES AND APPLICATIONS

F.W.H. KAMPERS, F.B.M. DUIVENVOORDEN, J.B.A.D. VAN ZON[*], P. BRINKGREVE[+], M.P.A. VIEGERS[*], D.C. KONINGSBERGER.

Laboratory for Inorganic Chemistry
+ Technological Development and Design Group and CTD
Eindhoven University of Technology
P.O. Box 513, 5600 MB Eindhoven, The Netherlands
* Philips Research Laboratories
P.O. Box 80000, 5600 JA Eindhoven, The Netherlands

In order to be independent of poor availability of synchrotron beamtime a laboratory EXAFS spectrometer has been developed. The X-ray source is a rotating anode generator (max. voltage 60 kV, max. current 300 mA). Monochromatisation and focusing is done with a linear spectrometer, based upon the Rowland circle geometry and a silicon crystal monochromator. High positioning accuracy of monochromator and sample stages are achieved by computer control and position feedback with magnetic rulers. Ionisation chambers monitor incoming and transmitted flux.
The spectra of Pt and $Na_2Pt(OH)_6$ and their Fourier transforms are compared with the same data taken at SSRL, Stanford (USA). The influence of the resolution on the Fourier transforms has been investigated. The applicability of the apparatus is demonstrated with 6 wt% Bi in $LaPO_4$ of which the oxygen coordination has been compared to that of Bi in $BiPO_4$. As a second example data of Platinum metal particles in ZSM-5 catalyst are presented.

1. INTRODUCTION

Reliable structural information with the EXAFS technique can only be obtained from high quality experimental data. In order to get a sufficient signal to noise ratio high intensity radiation is required. Synchrotron radiation is extremely suitable for EXAFS experiments. Disadvantages of the use of synchrotron radiation are: limited availability of beamtime, high cost and sometimes unreliable operation. A laboratory EXAFS system has been developed which enables collection of high quality EXAFS data. The principles of the apparatus will be outlined in the next section with a brief description of the equipment which is used. The performance of this spectrometer has been tested by comparing EXAFS data with measurements on the same samples carried out at Stanford Synchrotron Radiation Laboratory (SSRL). The applicability of the system will further be demonstrated with two examples: 2 wt% Bi in $LaPO_4$ and 3 wt% Pt in ZSM-5 zeolite catalyst.

2. PRINCIPLES OF THE LABORATORY EXAFS SYSTEM

The system makes use of a commercially available X-ray source, a linear spectrometer based upon the Rowland circle geometry with the X-ray source as fixed point and a diffraction crystal as monochromator. Ionisation chambers are used as detectors for the transmission EXAFS data. The acquisition of an EXAFS spectrum is automated and controlled by a computer.

2.1. The X-ray source

To obtain a high photon flux an Elliot GX-21 rotating anode X-ray generator (15 kW) is used (max. voltage: 60 kV; max. current: 300 mA; focal spot size: 0.5×10 mm^2; max. rotation speed: 6000 rpm). The main advantage of this generator is the possibility of an actual positioning of the electron focal spot on the Rowland circle of the spectrometer. Another advantage is the easy adjustibility of the cathode anode distance. By optimalisation of this distance it is possible to maximise the tube current (minimising space charge effects) at a certain

maximum value of the tube voltage. The maximum value is determined by the energy of the absorption edge of the sample to be measured and the type of monochromator crystal which is used because it has to be lower than the excitation energy of higher harmonic radiation which deteriorates the signal to noise ratio. The take-off angle is chosen to be 5.5°, as a compromise between spot width and brightness.

2.2 The linear Spectrometer

The radiation exits the tube as a polychromatic diverging beam. The Rowland circle geometry with a curved (Johann or Johansson type) monochromator crystal is used to obtain a high intensity monochromatic beam which is focussed on the sample. A linear spectrometer has been designed and constructed to maintain the Rowland circle geometry [1,2]. The positioning of the monochromator and the sample stage is computer controlled. The spectrometer has a positioning accuracy of $\pm$ 5 μm allowing an energy reproducibility of 0.1 eV at 9000 eV. The radius of the Rowland circle can freely be chosen. For the experiments described here a radius of 50 cm was used.

2.3 Monochromator Crystals

A perfect diffraction crystal is used as a narrow energy bandpass filter. Silicon Johann and Johansson type crystals of different orientations are used (Table 1).

TABLE 1
Common silicon crystal orientations

Orientation	Spacing	Energy range (keV)
111	3.1353	3.5 - 10
311	1.6374	7 - 19
400	1.3576	8 - 23

An advantage of the Si(111) and Si(311) crystals is that the second order reflection is forbidden. The next order reflection has an energy which is three times the energy of the chosen radiation. This means that the tube

voltage and consequently the current can be higher which yields larger intensities.

2.4 The detection system

To accurately measure the absorption coefficient it is necessary to measure the intensity of the (monochromatic) incoming and the transmitted beam. Since the EXAFS signal is only a fraction of the total absorption coefficient an accuracy of 10^{-3}-10^{-5} in the determination of the absorption coefficient is needed. So a high stability, low noise detector system is required. In addition to this, large intensity fluctuations in the incoming beam or in the transmitted beam when scanning through an absorption edge requires a detection system with a large dynamical range. Special designed ionisation chambers are used together with low noise current amplifiers. Within a large range of incident photon fluxes the number of counts is proportional to the number of photons absorbed in the active volume of the chambers.

2.5 Computer control

The acquisition of an EXAFS spectrum is fully automated and controlled by a PDP 11 compatible computer system. The central computer communicates with the microprocessors which control the movement of the monochromator and sample stages. A positioning feedback system is realised via magnetic ruler systems which determine the position of each stage with an accuracy of $\pm$ 5 μm.

3. PERFORMANCE

3.1 Comparison with synchrotron data

To determine the quality of the EXAFS data measured with the laboratory EXAFS spectrometer the EXAFS spectra of the Pt LIII-edge (11564 eV) of Pt metal foil and $Na_2Pt(OH)_6$ are compared with the data obtained on the same samples taken at S.S.R.L. (Stanford Synchrotron Radiation Laboratory, USA).

All spectra were collected at room temperature

A Si(400) Johann monochromator crystal was used on the laboratory spectrometer. The crystal was irradiated over an area of 10 mm (vertical)x 20 mm (horizontal). The measured resolution was about 14 eV at the Pt-LIII-edge. The x-ray generator operated at 21 kV and 240 mA. Data collection time for the Pt metal foil and the $Na_2Pt(OH)_6$ sample were 3 and 22 hrs respectively. The Stanford data were measured at EXAFS Station 1-5 (Electron energy 3 GeV; current 40 mA). A channel-cut Si(220) was used for monochromatisation giving an estimated resolution of 3-4 eV at 11 keV. The scantime for both samples was 35 min. It can be seen in Figure 1 that the signal to noise ratio of the spectra do not differ much showing that good quality EXAFS data can be obtained with a laboratory EXAFS facility. The differences at low k values are due to the lower resolution obtained with the Si(400) Johann monochromator in comparison to the SSRL Si(220) channel cut crystal.

3.2 The influence of the resolution on the EXAFS amplitude

In general it is essential to know which resolution is acceptable in order to derive reliable structural information from EXAFS data. With laboratory EXAFS in particular the influence of the resolution on the data is very important because resolution is often traded for intensity. The way in which the structural information contained in the EXAFS signal is affected by the energy resolution determines the maximum horizontal spot size allowed for EXAFS measurements with Johann type crystals.

In an EXAFS spectrum the distance between the nodes in energy-space of the EXAFS decreases with increasing coordination distances. This means that with a certain energy resolution higher coordination shells are affected more strongly. The backscattering amplitude of low Z elements decreases faster with k than of high Z elements. This implicates that the EXAFS information of higher coordination shells consisting of low Z elements gets unreliable faster than for high elements. This is demonstrated by simulating poor resolution in calculated EXAFS spectra. The measured EXAFS function $\chi'(E)$ is a convolution of the actual function $\chi(E)$ with an energy resolution function $g(E)$. The convolution is given by

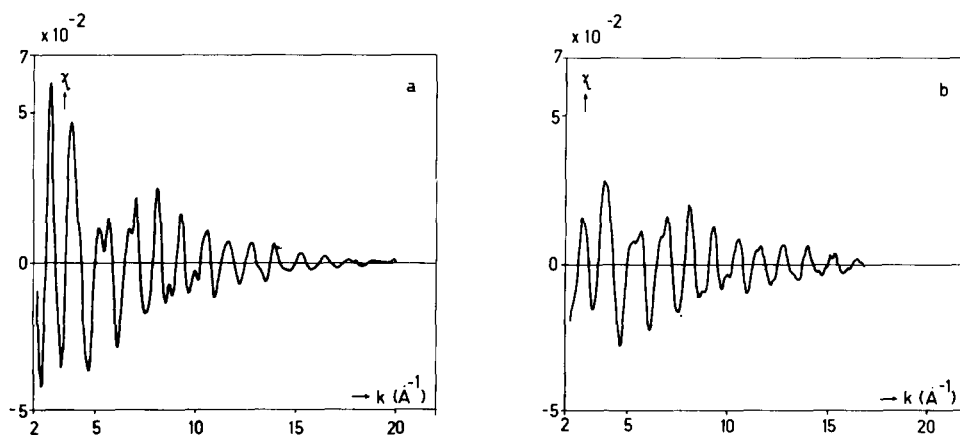$$\chi'(E) = \int_{-\infty}^{+\infty} g(E,E') \, \chi(E')dE'.$$

FIGURE 1
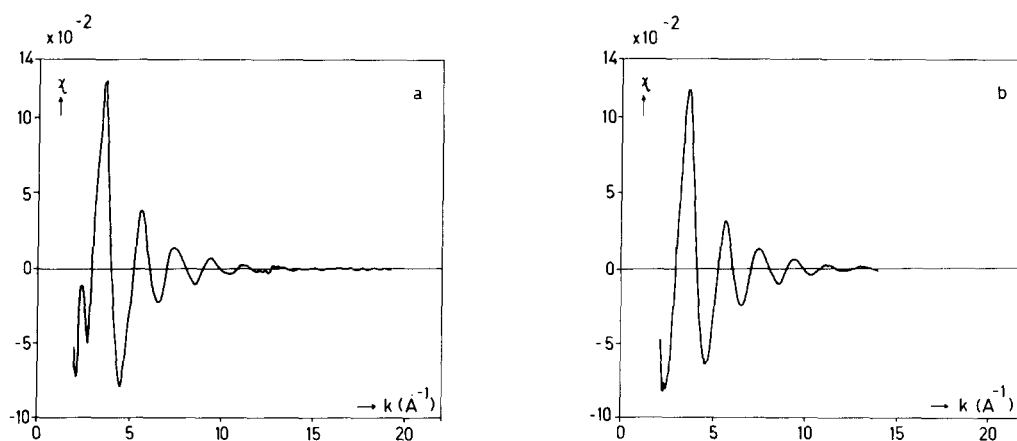EXAFS spectra of Pt foil from Stanford (a), from Eindhoven (b).

FIGURE 2
EXAFS spectra of $Na_2Pt(OH)_6$ from Stanford (a), from Eindhoven (b).

Actual EXAFS functions of a Pt-Pt and of a Pt-O absorber-scatterer pair are calculated using the phase and amplitude functions obtained by backtransformation of the first shell of Pt-foil and $Na_2Pt(OH)_6$ (fig. 2). Pt-foil and $Na_2Pt(OH)_6$ data were taken at SSRL.

The experimental energy resolution is simulated with a Gaussian type resolution function given by

$$g(E,E') = \frac{1}{\sqrt{2\pi \ \tau^2}} \ e^{-\frac{(E'-E)^2}{2\tau^2}}$$

The FWHM of this function is $2\sqrt{2\ln 2} \cdot \tau$. The results of the convolutions for two different τ values are given in figure 3 with dotted lines. The thus obtained Pt-Pt and Pt-O EXAFS functions are Fourier transformed (with phase correction) to show the influence of resolution on the peaks corresponding with the different coordinations.

The results are summarized in Table 2. Reliable structural information in most cases can still be obtained with an experimental resolution of about 20 eV. However, for low Z scatterers at higher coordination distances better resolutions are necessary.

4. APPLICATIONS

4.1 The position of the Bi^{3+}-ion in the lattice of α-LaPO$_4$.
(In cooperation with G. Blasse and M. Oomen, University of Utrecht)

An EXAFS investigation was started to determine the local structure around the Bi^{3+}-ion present in a α-LaPO$_4$ lattice in small concentrations (6 wt%). The position of the Bi^{3+}-ion in this lattice is probably connected with the luminescence properties. It might be possible
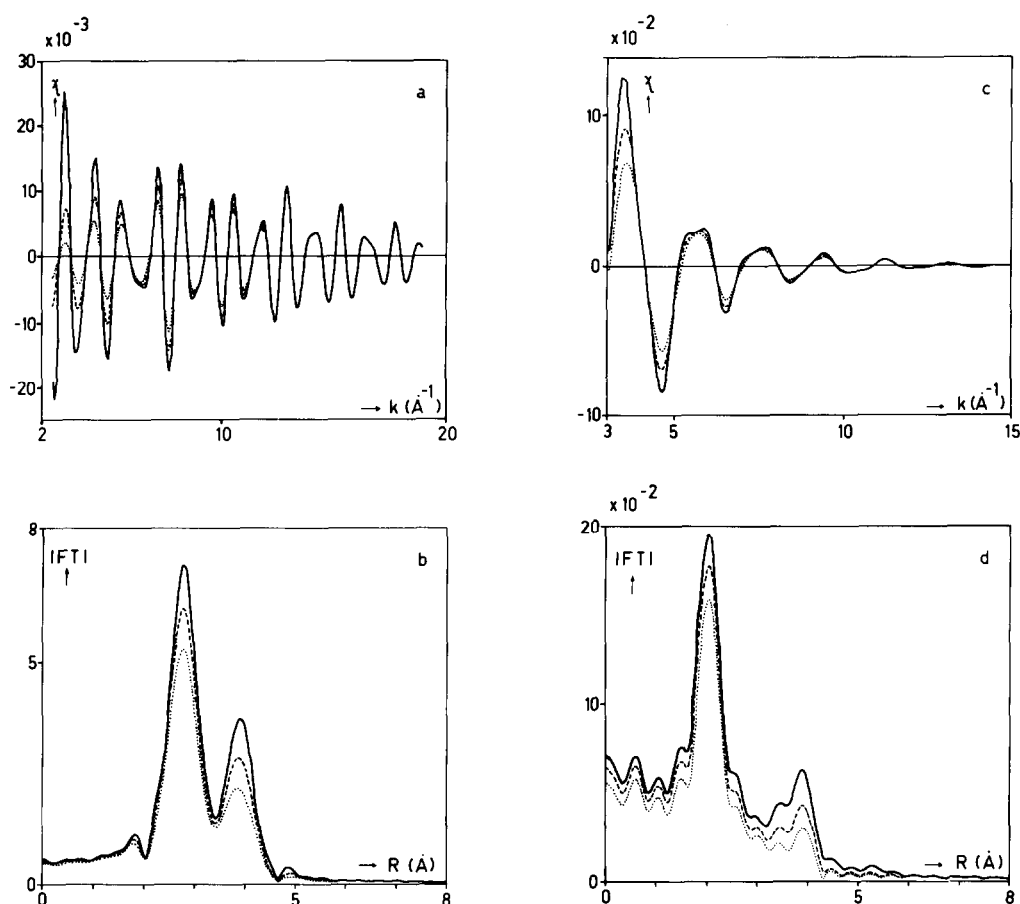
TABLE 2
Results of the convolutions of the calculated EXAFS spectra (R: coordination distance, $2\sqrt{2\ln 2} \cdot \tau$: FWHM).

Calculated EXAFS	τ (eV)	Peak height decrease in R-space (%)
Pt-Pt R=2.77 Å	6	13.7
	9	26.2
R=4.00 Å	6	23.6
	9	41.6
Pt-O R=2.05 Å	6	9.2
	9	18.8
R=4.00 Å	6	30.3
	9	51.3

FIGURE 3

Calculated two coordination shell EXAFS spectra ((——): no convolution, (---): convoluted with τ = 6 eV, (   ): convoluted with τ = 9 eV) and their Fourier Transforms (N: coordination number, R: coordination distance, $\Delta\sigma^2$: Debye-Waller factor, V_0: inner potential).

(a) Pt-Pt
N=5, R=2.77 Å, $\Delta\sigma^2$=0, V_0=0
N=5, R=4.00 Å, $\Delta\sigma^2$=0, V_0^0=0

(b) k^3 Fourier Transform of (a),
Δk = 2.76 - 11.42 Å^{-1}
(Pt-Pt phase corrected)

(c) Pt-O
N=6, R=2.05 Å, $\Delta\sigma^2$=0, V_0=0
N=6, R=4.00 Å, $\Delta\sigma^2$=0, V_0^0=0

(d) k^1 Fourier Transform of (c)
Δk = 4.21 - 11.73 Å^{-1}
(Pt-O phase corrected)

that Bi^{3+}, when replacing La^{3+} takes an off-centre position. The oxygen coordination of La^{3+} in α-LaPO$_4$ is as follows: N=4, R=2.35 Å, and N=4, R=2.68 Å. (Average coordination distance: R=2.515 Å).

EXAFS measurements on the LIII-edge of Bismuth (13418 eV) have been carried out to find the coordination parameters of the first shell

oxygen neighbours of the Bi^{3+}-ion in LaPO$_4$. (The EXAFS spectrum of a Bi in α-LaPO$_4$ sample, diluted with Al$_2$O$_3$ - 2 wt% Bi after mixing - measured at room temperature is shown in Fig. 4a. The scantime was 7 hours. The resolution at 13000 eV with the Johann type Si(400) monochromator was 20 eV (crystal area width: 20 mm, height: 10 mm).
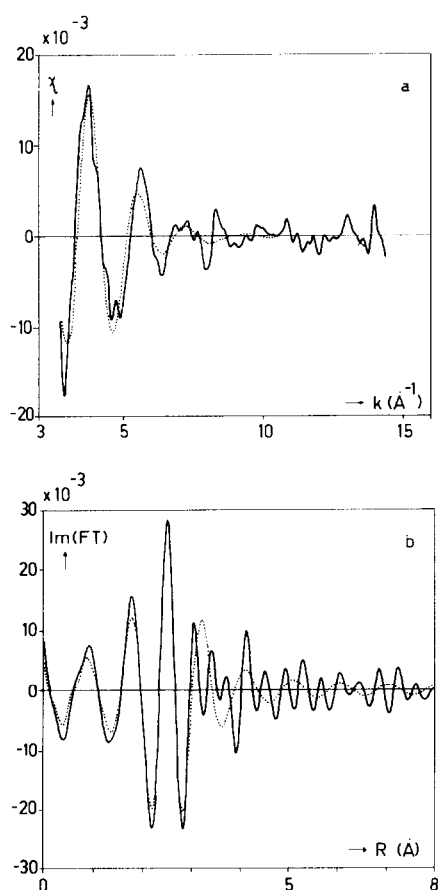
To analyse this spectrum reliable information

FIGURE 4

4(a) EXAFS function of Bi in α-LaPO₄
    —— experiment, ··· calculation (see table
    3a)
4(b) Fourier transform (imaginary part) of the
    Bi in α-LaPO₄ EXAFS experiment (k^1, k-range
    3.30-10.0 A⁻¹,——)and best fit (k^1, k-range
    3.37-10.0 A⁻¹, •••)

about the phase shift and backscattering ampli-
tude is necessary for the Bi-O absorber-scatter-
er combination. In this case, Bi substituted
$ScBO_3$ was used. The first coordination shell
consists of 6 oxygen neighbours, all at a dis-
tance of 2.36 A. The reliability of Bi in $ScBO_3$
as a reference was tested by analysing the EXAFS
data of α-Bi_2O_3, of which the crystal structure
is known. Experimental and calculated EXAFS show-
ed a good fit.

α-$BiPO_4$ and α-$LaPO_4$ are isomorphous materials

with slightly different lattice parameters. The
oxygen coordination of Bi^{3+} in α-$BiPO_4$ is: N=4,
R= 2.33 A and N=4, R= 2.66 A (average coordinat-
ion distance: R= 2.495 A). Fig. 5a shows the ex-
perimental EXAFS spectrum of the LIII-edge of
of Bi in α-$BiPO_4$. The Bi-O phase corrected
Fourier transform of the experimental data is
given in fig. 5b. The maximum of the imaginary
part is reached for the average Bi-O coordinat-
ion distance R= 2.49 A.
A Bi-O EXAFS function calculated with the para-
meters given in table 3a (using the phase and
amplitude functions obtained from the Bi-$ScBO_3$
reference) gives the best fit with the experi-
mental EXAFS spectrum (fig. 5a, dotted line).
The Bi-O phase corrected Fourier transform of
this fit is for 1.5<R<3 A identical with that
of the experimental data (see fig. 5b, dotted
line). The EXAFS results are thus in agreement
with the crystallographic data of α-$BiPO_4$.

A Bi-O phase corrected Fourier transform of
an EXAFS function calculated with the parameters
given in table 3b also shows a good agreement
with the experiment on Bi in α-$LaPO_4$. The average
Bi-O coordination distance is 2.54 A, which is
0.025 A larger than the average La-O coordina-
tion distance.

The Debye-Waller factor of the Bi-O pair in
α-$LaPO_4$ is also larger (0.0032 A^2) than in the
α-$BiPO_4$ lattice, which results in a smaller Bi-O
peak (see fig. 6). Both results point to the
possibility of a slight off-centre position of
Bi^{3+} in $LaPO_4$. More experiments are needed to

TABLE 3
Parameters used in calculating a Bi-O EXAFS
function (N: coordination number, R: coordina-
tion distance, $\Delta\sigma^2$: Debye-Waller factor,
V_0: inner potential).

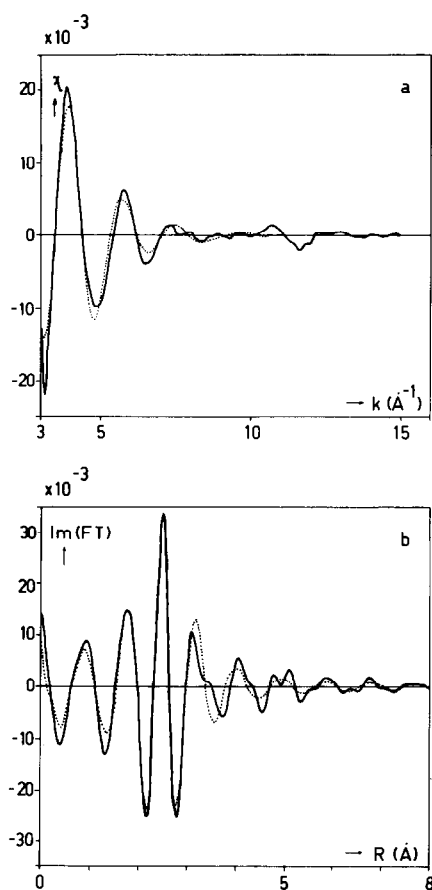| Sample	N	R(A)	$\Delta\sigma^2$(A^2)	V_0(eV)
(a) α-$BiPO_4$	8	2.49	0.0033	+3.8
(b) Bi-$LaPO_4$ (6 wt%)	8	2.54	0.0065	-2.3

FIGURE 5

5(a) EXAFS function of Bi in α-BiPO$_4$
— experiment, ••• calculation (see table 3a.

5(b) Fourier transform (imaginary part) of the Bi in α-BiPO$_4$ EXAFS experiment (k^1, Δk 3.24-10.0 A^{-1}—) and best fit (k^1, Δk 3.47-10.0 A^{-1},°°°).

FIGURE 6

Fourier transform (magnitude) of EXAFS experiments on Bi in α-BiPO$_4$ (k^1, Δk 3.24-10.0 A^{-1},—) and Bi in α-LaPO$_4$ (k^1, Δk 3.30-10.0 A^{-1},°°°)

further verify these results.

4.2 Platinum metal crystallites in ZSM-5

Together with A. Miecznikowski, C. Engelen and J. van Hooff an EXAFS study on Pt loaded-ZSM-5 was started. The influence of the method of preparation of the Pt-ZSM-5 catalyst on the size of the platinum metal crystallites was investigated. Also a point of interest is the influence of the preparation method on the position of the metal crystallites in the ZSM-5
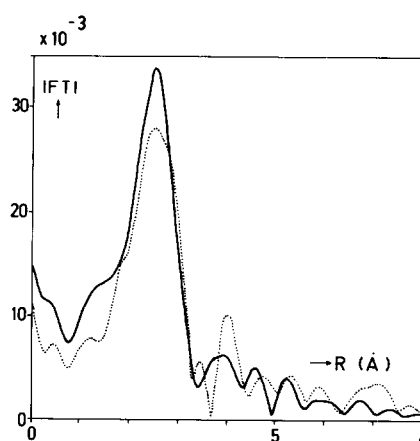
catalysts (Outside and/or inside the pores).

A zeolite ZSM-5 (Si/Al=40, orthorhombic structure) was used as support. The platinum was introduced as Pt(NH$_3$)$_4^{2-}$ by impregnation of H-ZSM-5 both at RT. The catalysts were dried at 100°C for 20 hrs and calcinated in a mixture O$_2$/He = 20/80 at 250°C with the temperature being increased from RT to 350°C at a rate of 1°C/min. Reduction was carried out in flowing hydrogen at 350°C (heating rate 5°C/min).

EXAFS measurements were carried out on the Pt LIII-edge at RT after passivation (cooling down in flowing H$_2$ and at RT slowly introducing a mixture of O$_2$ and He) of the catalysts. The resolution of the Si(400) Johann crystal at the platinum edge was 14 eV (V= 10 mm, h= 20mm), with a scantime of 22 hrs. The EXAFS spectra of both a 3 wt% (via ion-exchange) and a 5 wt% (via impregnation) Pt/ZSM-5 catalyst are displayed in.Figure 7. Since it is likely, that the platinum metal particles are partly oxidized a k^3-weighted Pt-Pt phase and amplitude corrected Fourier transform gives the best separation between the Pt-Pt and the Pt-O bonds. (see Figure 8). In a Pt-Pt phase corrected Fourier transform the Pt-Pt contribution peaks at the
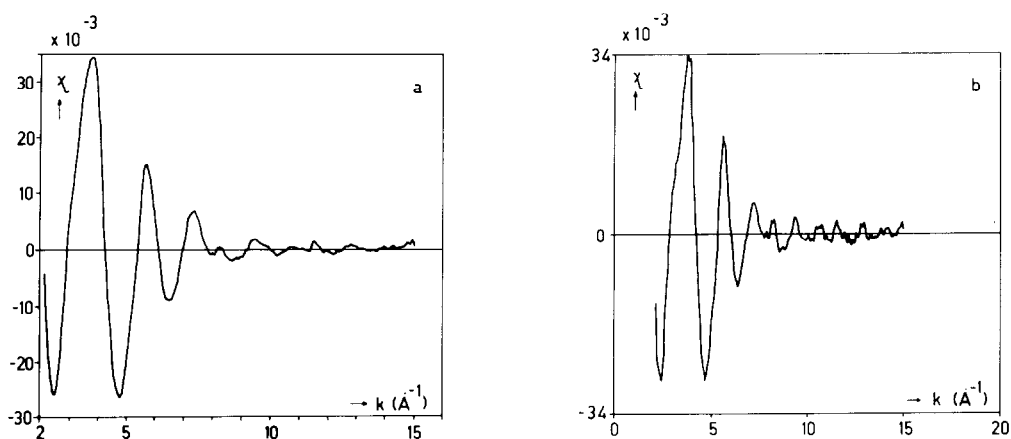
FIGURE 7
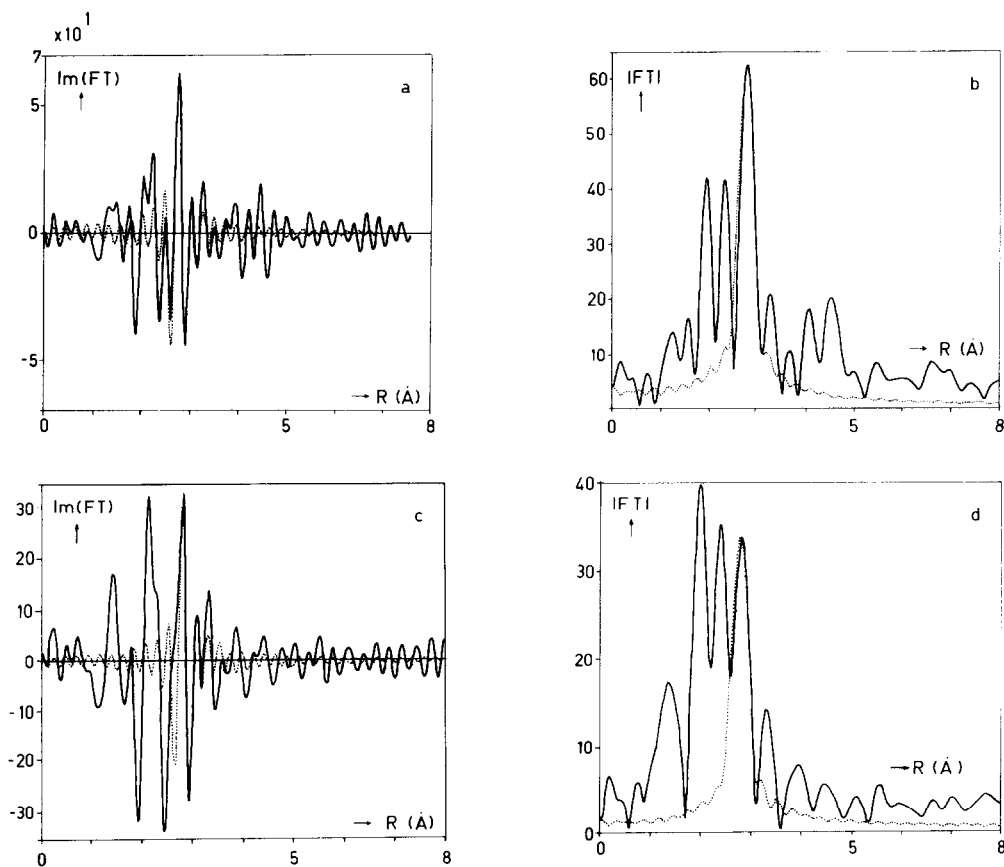EXAFS spectra of 3 wt% Pt/H-ZSM-5 (ion-exchange) (a) and of 5 wt% Pt/H-ZSM-5 (impregnation) (b).

FIGURE 8
Pt-Pt phase and amplitude corrected Fourier Transforms (k^3, Δk = 2.9 - 14 Å^{-1}) (imaginary part and magnitude) of 3 wt% Pt/H-ZSM-5 (a,b) and of 5 wt% Pt/H-ZSM-5 (c,d). The Pt-Pt contributions are indicated by dotted lines.

TABLE 4
Coordination parameters

Pt-Pt coordination	N	R (Å)	$\Delta\sigma^2$ ($Å^2$)
Impregnation (5 wt%)	5.5	2.77	0.003
Ion-exchange (3 wt%)	2.9	2.77	0.003

actual coordination distance (in both transforms of both catalysts: at 2.77 Å). The Fourier transform (Pt-Pt phase and amplitude corrected) of an EXAFS function calculated with the coordination parameters as given in Table 4, gives for both catalysts a Pt-Pt peak which superimposes the Pt-Pt peak in the Fourier transform of the experimental data.

Further analysis and in-situ measurements are needed in order to derive definite conclus-

ions about the structural properties of the Pt/ZSM-5 catalytic system. However, it can certainly be concluded from the results reported here that the impregnation method leads to larger platinum crystallites on the ZSM-5 support.

REFERENCES

1. J.B.A.D. van Zon, Extended X-ray Absorption Fine Structure Spectroscopy: Design of a Spectrometer and Application to Rhodium Supported on Alumina Catalysts (Thesis, Eindhoven University of Technology, 1984).
2. P.Brinkgreve, T.M.J.Maas, D.C.Koningsberger, J.B.A.D.van Zon, M.H.C.Janssen, A.C.M.E. van Kalmthout and M.P.A.Viegers, A Linear Spectrometer Designed for EXAFS Spectroscopy, in: EXAFS and Near Edge Structures III, eds. K.O.Hodgson, B.Hedman and J.E. Penner-Hahn (Springer Verlag Berlin, 1984).